(Phys. Rev. A, accepted)

Image states in metal clusters

Patrick Rinke,[1,*] Kris Delaney,[1,†] P. García-González,[2,‡] and R. W. Godby[1]

[1]*Department of Physics, University of York, Heslington, York YO10 5DD, United Kingdom*
[2]*Departamento de Física de la Materia Condensada, Universidad Autónoma de Madrid, E-28049, Madrid, Spain*

(Dated: February 2, 2008)

The existence of image states in small clusters is shown, using a quantum-mechanical many-body approach. We present image state energies and wave functions for spherical jellium clusters up to 186 atoms, calculated in the *GW* approximation, where G is the Green's function, and W the dynamically screened Coulomb interaction, which by construction contains the dynamic long-range correlation effects that give rise to image effects. In addition we find that image states are also subject to quantum confinement. To extrapolate our investigations to clusters in the mesoscopic size range, we propose a semiclassical model potential, which we test against our full *GW* results.

PACS numbers: 36.40.Cg, 73.20.At, 73.22.Dj

I. INTRODUCTION

Image states are highly extended, excited electronic states that occur predominantly at the surface of a polarizable material when an extra electron is added to the system. Electrons in such an image state feel the attractive force of the charge induced in the material even far away from the surface due to the extremely long-ranged correlation of the Coulomb potential.

In the past, research on image states was mostly devoted to metal surfaces, both experimentally [1] and theoretically [2]. Recently, however, studies have also been extended to nanotubes [3] and metallic nanowires on surfaces [4]. Unlike surfaces, isolated nanoclusters are not stationary and image states can therefore only be resolved indirectly with the experimental techniques currently available. By measuring the capture cross section of low-energy electrons, for instance, Kasperovich *et al.* were able to identify a clear signature of image effects in free sodium clusters of 4 nm radius [5].

In the context of water clusters, polar molecules, and clusters of rare gas atoms, excess electron states have been widely discussed in the literature [6]. The electron-electron interaction in these clusters is typically included using quasiclassical dielectric screening, which becomes justified in the mesoscopic regime but is not parameter-free [7, 8, 9]. For smaller clusters, the interaction of the excess electron with the cluster has been modeled using electron-atom pseudopotentials, with the ground state geometry from molecular dynamics [10]; image states were not included in the study.

While the effect of the cluster polarization potential on the scattering [11] and capture [12] cross section has been studied with a variety of different approaches, we will focus in this paper specifically on the bound states that arise from the interaction of the excess electron with its image charges. We report first-principles calculations for jellium clusters with sodium densities as a prototype system for isolated nanoclusters. The Coulomb interaction between all valence electrons is taken into account in the framework of many-body perturbation theory. The image state energies and wave functions were obtained using the *GW* approximation [13], which has proven to be very successful for the description of image effects [2, 14, 15] and other quasiparticle properties [16]. Our calculations predict the existence of image states in these zero-dimensional nanostructures even down to relatively small cluster sizes.

By way of illustration, the classical image potential outside a neutral solid sphere with radius R_c and dielectric constant ε has the form [17]

$$v_{\rm im}^{c}(r) = \sum_{n=1}^{\infty} \frac{-n(\varepsilon-1)}{2n(\varepsilon+1)+2} \frac{R_c^{2n+1}}{r^{2n+2}} \approx \frac{-R_c^3}{2r^2(r^2-R_c^2)} \quad (1)$$

for $r > R_c$. The last expression illustrates the limit of a perfectly conducting sphere ($\varepsilon \to \infty$); the familar image potential of a flat surface, $-1/4z$ where $z = r - R_c$, is recovered for large cluster radii.

The image potential for a solid sphere (1) decays asymptotically as $-1/r^4$ and thus much more rapidly than the image potential of the planar surface. However, in a region of size of order R_c just outside the surface, the much more accommodating flat-surface form prevails (Fig. 1).

As previously reported [3] the image potential of a metallic tube with radius R_t decays asymptotically as $-1/[rR_t \ln(r/R_t)]$ and is thus effectively situated closer to the flat-surface limit in Fig. 1. For both the cluster and the tube, the image potential depends on the radius of the nanostructure. For clusters, this dependence is

*Present address: Fritz-Haber-Institut der Max-Planck-Gesellschaft, Faradayweg 4–6, 14195 Berlin, Germany
†Present address: Department of Physics, University of Illinois at Urbana-Champaign, Urbana IL 61801-3080, USA
‡Present address: Departamento de Física Fundamental, UNED, Apartdado 60141, E-28080 Madrid, Spain

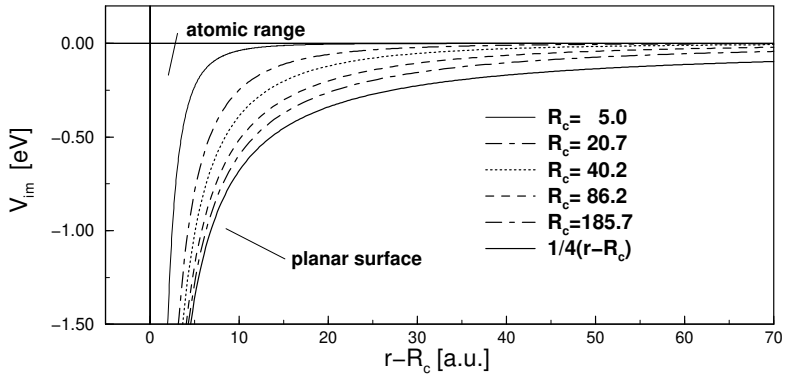

FIG. 1: The classical image potential, $v^c_{\rm im}(r)$ [Eq. 1], of a solid sphere with $\varepsilon = 1000$ becomes more accommodating with increasing radius R_c (in a.u.) and is bound by the planar surface (solid line to the right) and the atomic limit (solid line to the left).

considerable, as Fig. 1 illustrates, and consequently has a strong effect on the binding energy and the wave functions of the image states, as we will show in the following.

II. COMPUTATIONAL APPROACH

The quasiparticle energies and wave functions are formally the solution of the quasiparticle equation

$$\hat{H}_0\,\psi_n(\mathbf{r}) + \int d\mathbf{r}'\Sigma(\mathbf{r},\mathbf{r}';\epsilon_n)\psi_n(\mathbf{r}') = \epsilon_n\psi_n(\mathbf{r}) \qquad (2)$$

with the effective one-particle Hamiltonian, $\hat{H}_0$, including the Hartree and the external potential. The nonlocal, dynamical self-energy $\Sigma(\mathbf{r},\mathbf{r}';\omega)$ contains the electron exchange and correlation effects beyond the Hartree mean-field and is, in the GW approximation, given by $\Sigma = GW$ [13], where G is the Green's function, and W the dynamically screened Coulomb interaction.

In the jellium clusters studied in this paper, the atomic nuclei are replaced by a homogeneous, positive background charge, $\rho^+(r) = \rho_0\Theta(R_c - r)$, with $\rho_0 = 3/4\pi r_s$. The Wigner-Seitz radius r_s is indicative of the electron density of the material and we chose a value of r_s=4.0 for the jellium clusters with sodium densities presented here.

The electrostatic potential created by the background charge density, $\rho^+(r)$, is spherically symmetric and, therefore, all cross section planes through the origin of the cluster are equivalent. It is thus sufficient to describe the system by two radial coordinates r and r' and one angular coordinate θ that denotes the angle between the vectors $\mathbf{r}$ and $\mathbf{r}'$. The self-energy then assumes the much simpler form $\Sigma(r,r',\theta;\omega) = \sum_{l=0}^{\infty}\left[\Sigma^x_l(r,r') + \Sigma^c_l(r,r';\omega)\right]P_l(\cos\theta)$.

The Legendre expansion coefficients of the exchange, Σ^x_l, and the correlation part, Σ^c_l, of the self-energy are calculated directly, thereby surpassing the need for an explicit treatment of the angular dependence. We use a real-space and imaginary time representation [18] to calculate the self-energy from the Kohn-Sham Green's function of a preceding density-functional calculation in the local density approximation (LDA). The expression for the self-energy on the real frequency axis is obtained by means of analytic continuation [18].

To obtain the quasiparticle energies and wave functions, the quasiparticle equation (2) is fully diagonalized in the basis of the LDA wave functions. The ionization potential and the electron affinities calculated in this way agree well with available data from photoionization experiments [19] and are also in excellent agreement with the only previous GW study on spherical jellium clusters by Saito *et al* [20], in which a plasmon pole model was used. The energy range in which surface and image states occur in jellium clusters, however, was not included in their investigation.

III. IMAGE STATES IN METAL CLUSTERS

In Fig. 2 we present the highest image state [21] calculated for the clusters Na_{138} and Na_{186}, respectively [22]. Both image states are very similar in character and extend extremely far into the vacuum having an almost insignificant overlap with the cluster. Most strikingly, however, is that the corresponding LDA states bear no resemblance to the image state wave functions. Due to the absence of long-range correlation effects in density-functional theory (DFT) the corresponding state in the LDA calculation becomes an unbound state that is scattered by the effective potential. This observation proves that a full diagonalization of the quasiparticle Hamiltonian (2) is necessary, because the LDA wave functions no longer provide a good description of the quasiparticle wave functions, as is the case for bulk [23] and low lying cluster [20, 24] states. The exchange-correlation potential in the LDA decays exponentially in the vacuum region as opposed to the $-1/r^4$ behavior of the image potential felt by an extra electron. The similarity between these two potentials for small clusters is coincidental and leads in certain cases to bound image states even in the LDA (see Fig. 3).

Owing to the much more rapid decay of the image potential for a solid sphere (1), the energy band in which image states are found is reduced to ∼0.2 eV below the vacuum level for a small cluster compared to an energy range of approximately 1 eV found at metal surfaces [2].

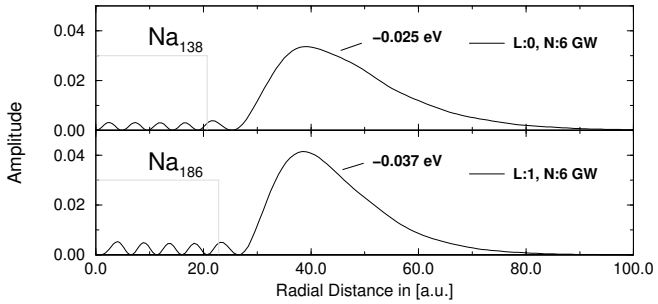

FIG. 2: For each of the clusters Na_{138} and Na_{186}, a loosely bound image state is found that predominantly resides in the vacuum region outside the cluster and has very little overlap with the cluster region. In the LDA, neither an image state nor a bound state with the same quantum numbers can be obtained. (The energies are referenced with respect to the vacuum and the gray box marks the extent of the clusters.)

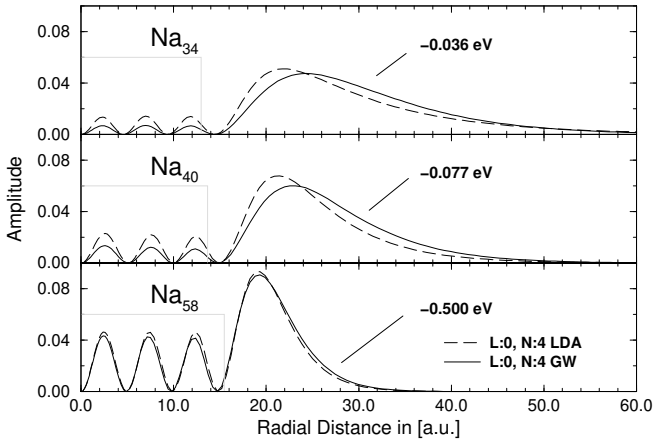

FIG. 3: The highest image state (solid line) in Na_{34} becomes more tightly bound and more strongly localized with increasing cluster size, Na_{40}, and eventually evolves into a surface resonance in Na_{58}. For comparison, the LDA wave functions have been included (dashed lines).

The image state binding energies of -0.025 eV for Na_{138} and -0.037 eV for Na_{186} are thus small in relation to energies of a few tenths of an eV observed for sodium surfaces [2]. For larger clusters, the overlap of the higher image states with the cluster region becomes negligible (see Fig. 2). We therefore expect these states to be insensitive to any atomic structure of the cluster, and to be long lived.

Focusing on the highest image state in the sodium cluster series, we now demonstrate that image states are subject to quantum confinement effects. In Fig. 3, we have illustrated the evolution of the state (L=0,N=4) with increasing cluster size. In the smallest cluster, Na_{34}, the image state is most narrowly bound at only -0.036 eV, whereas in the next larger cluster, Na_{40}, it is localized closer to the surface and exhibits more overlap with the cluster itself. The same state has evolved into a surface resonance for the Na_{58} cluster and will eventually become an ordinary bound cluster state for larger quantum dots. This size dependence of the image states results from a delicate interplay between the confinement of the cluster potential and the long range of the image potential. If there was no overlap of the image state wave function with the cluster region, as assumed in many classical approaches, then the image states in the size range depicted in Fig. 3 would be identical, since the variation of the image potential itself can be regarded as negligible in this range (see Fig. 1). In reality, however, the overlap with the cluster increases with cluster size, as can be seen in Fig. 3, which is accompanied by an increase in binding energy. Subsequently, the electron in the image state will sample less and less of the long-ranging image tail. A reduced confinement by the external cluster potential will therefore lead to a stronger confinement by the image potential and thus to a stronger localization overall.

Furthermore, Na_{34} is the smallest cluster in the sodium series for which at least one image state is bound. This observation therefore positively answers the question that arises from Eq. (1) and Fig. 1 if there exists a minimum cluster size for image effects to become important.

Experimentally it has recently been demonstrated by Kasperovich *et al.* [5] that the size of sodium nanoclusters can be determined by measuring the contribution to the capture cross section that arises from image effects. In this context we therefore like to emphasize that, in contrast to surfaces, spherical nanostructures provide an extra parameter to tailor the binding energy and the shape of an images state.

IV. TOWARDS THE MESOSCOPIC SIZE RANGE

In the final part of this paper we will pursue the notion of incorporating image effects into a suitable model potential in the framework of our DFT calculations, in order to predict image states for clusters in the mesoscopic size range. Our full *GW* results will thereby serve as a reference to establish the validity of the model and to give an estimate of its transferability.

Because the exchange-correlation potential in the LDA $v_{xc}(r)$ is proportional to a power of the electron density, it will decay exponentially outside the cluster. The image potential (1) on the other hand is long ranging since it asymptotically follows an inverse power-law behavior that varies between $-1/r^4$ for small clusters and $-1/r$ for larger ones. In the vicinity of the cluster surface, the exponentially decaying $v_{xc}(r)$ will thus be shallower than the image potential, which then approaches zero much more slowly after a crossover point with the LDA potential (see Fig. 4).

In the spirit of image state calculations for surfaces performed by Serena *et al.* and Chulkov *et at.* [25], who apply model potentials to correct the erroneous decay of the Kohn-Sham exchange-correlation potential, we have

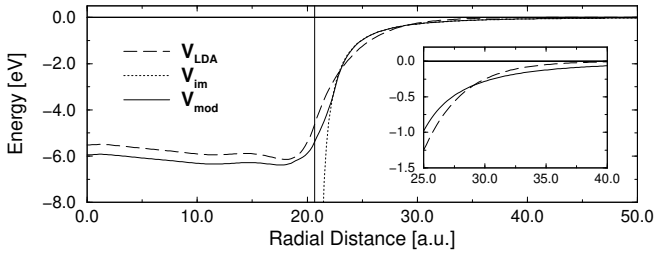

FIG. 4: The model potential of Eq. (3) of a Na_{138} cluster with $\varepsilon = 1000$ (solid line) crosses over with the exponentially decaying LDA-v_{xc} potential (dashed line) and follows the inverse power law decay of the classical image potential (Eq. (1)) (dotted line) by construction.

constructed an effective potential

$$v_{\rm mod}(r,\varepsilon) = \begin{cases} v_{xc}(r) & r < R_c - d \\ p(r) & R_c - d < r < R_c + d \\ v^c_{\rm im}(r,\varepsilon) & R_c + d < r \end{cases} \quad (3)$$

for our jellium clusters, based on the classical image potential of a solid sphere (1). The model potential is designed to be local, so that it can be employed on the level of our DFT-LDA calculations. The interpolation function $p(r)$ is a third-order polynomial which joins smoothly and continuously onto v_{xc} and $v_{\rm im}$ at $r = R_c \pm d$. For the value of d we impose the constraint $v_{xc}(R_c - d) < v^c_{\rm im}(R_c + d)$ in order to avoid an unphysical shape of the potential in the intermediate region. Because the occupied wave functions and thus the density might be slightly altered by the modifications, we determine the model potential self-consistently, applying Eq. (3) at every iteration of the density.

In Fig. 4 we present the model potential obtained for the Na_{138} cluster and a dielectric constant of $\varepsilon = 1000$. Inside the cluster, the model potential follows the shape of the LDA-v_{xc} potential, but in the immediate vicinity of the cluster surface it approaches zero much faster. At a distance of approximately one-half the cluster radius away from the surface the model potential, which by construction follows the inverse power-law decay of the classical image potential, $v^c_{\rm im}(r)$, crosses over with the exponentially decaying exchange-correlation potential in the LDA, as expected.

The inclusion of long-range correlation effects in this fashion proves to be necessary to reproduce the same image states as our full quasiparticle calculations, in particular in those cases where the LDA breaks down (see Fig. 2). The shape of the image state wave functions and the energies dependend on the dielectric constant, while the *number* of such states is insensitive to it.

To close the discussion on our model potential, we apply it to a cluster approaching the mesoscopic size range. For this purpose we chose the cluster Na_{508}, that has a radius of 31.9 a.u.. Our model potential calculation yields six image states, whereas only three of them have a corresponding state in the LDA. The highest image state predicted by the model is very narrowly bound (−0.004 eV). It extends extremely far into the vacuum and reaches its intensity maximum as far as two cluster radii away from the surface. This observation corroborates the conjecture that the number of image states increases for larger clusters until the familiar Rydberg series is recovered in the limit of infinitely large clusters. It further suggests that clusters with 2.5 times this radius, as those studied experimentally by Kasperovich *et al.* [5] (see also line for 86.2 a.u. in Fig. 1) will already bind a considerable number of image states, which will then contribute noticeably to the electron capture rate, as observed in the experiment [5].

V. CONCLUSIONS

In conclusion, we have presented image states for small clusters from a full quantum-mechanical many-body calculation. In contrast to surfaces, nanoclusters contain a finite number of image states, that are subject to quantum confinement effects. In order to describe image states in the *GW* approximation correctly, a full diagonalization of the quasiparticle Hamiltonian is necessary, because the LDA wave functions no longer provide a good description of the quasiparticle wave functions. To extend the discussion to mesoscopic clusters, we have devised a model potential that captures the correct asymptotic decay of the image potential and yields images states in qualitative agreement with the quasiparticle states of our *GW* approach.

Acknowledgments

We thank Wolf-Dieter Schöne, Peter Bokes, Tim Gould, and Héctor Mera for many fruitful discussions. This work was supported by the EPSRC and by the EU through the NANOPHASE Research Training Network (Contract No. HPRN-CT-2000-00167) and in part by the NANOQUANTA Network of Excellence (NMP4-CT-2004-500198). Patrick Rinke also acknowledges the support of the DAAD.

[1] K. Giesen, F. Hage, F.J. Himpsel, H.J. Riess and W. Steinmann, Phys. Rev. Lett. **55**, 300 (1985); G. Binning, K. H. Frank, H. Fuchs, N. Garcia, B. Reihl, H. Rohrer, F. Salvan and A. R. Williams, *ibid.* **55**, 991 (1985); R.W.

Schoenlein, J.G. Fujimoto, G.L. Eesely and T.W. Capehart, *ibid.* **61**, 2596 (1988); U. Höfer, I.L. Shumay, Ch. Reuss, U. Thomann, W. Wallauer and Th. Fauster, Science **277**, 1480 (1997).

[2] V.M. Silkin, E.V. Chulkov and P.M. Echenique, Surf. Sci. **437**, 330 (1999).

[3] B. E. Granger, P. Král, H.R. Sadeghpour and M. Shapiro, Phys. Rev. Lett. **89**, 135506 (2002).

[4] I. G. Hill and A. B. McLean, Phys. Rev. Lett. **82**, 2155 (1999).

[5] V. Kasperovich, K. Wong, G. Tikhonov and V.V. Kresin, Phys. Rev. Lett. **85**, 2729 (2000).

[6] P. Stampfli, Phys. Rep. **255**, 1 (1995) and references therein.

[7] M. Rosenblit and J. Jortner, J. Phys. Chem. **98**, 9365 (1994); J. Chem. Phys. **101**, 8039 (1994).

[8] V. M. Nabutovskii and D. A. Romanov, Sov. J. Low Temp. Phys. **11**, 277 (1985); Sov. Phys. JETP **63**, 133 (1986).

[9] G. Mo, C. C. Sung and R. H. Ritchie, Chem. Phys. Lett. **176**, 433 (1991).

[10] R. N. Barnett, U. Landman, Guy Makov and A. Nitzan, J. Chem. Phys. **93**, 6226 (1990); R. N. Barnett, U. Landman, C. L. Cleveland and J. Jortner, Phys. Rev. Lett. **59**, 811 (1987); R. N. Barnett, U. Landman, G. Rajagopal and A. Nitzan, Isr. J. Chem. **30**, 85 (1990); G. Rajagopal, R. N. Barnett, A. Nitzan, U. Landman, E. C. Honea, P. Labastie, M. L. Homer and R. L. Whetten, Phys. Rev. Lett. **64**, 2933 (1990).

[11] A. N. Ipatov, V. K. Ivanov, B. D. Agap'ev and W. Ekardt, J. Phys. B **31**, 925 (1998); P. Descourt, M. Farine and C. Guet, *ibid.* **33**, 4565 (2000).

[12] M. Bernath, O. Dragun, M. R. Spinella, H. Massmann and J. H. Pacheco, Phys. Rev. A **52**, 2173 (1995); P.-H. Hervieux, M. E. Madjet and H. Benali, *ibid.* **65**, 023202 (2002).

[13] L. Hedin, Phys. Rev. A **139**, 796 (1965).

[14] J. J. Deisz, A. G. Eguiluz and W. Hanke, Phys. Rev. Lett. **71**, 2793 (1993); I.D. White, R.W. Godby, M. M. Rieger and R.J. Needs, *ibid.* **80**, 4265 (1998).

[15] G. Fratesi, G.P. Brivio, P. Rinke and R.W. Godby, Phys. Rev. B **68**, 195404 (2003).

[16] W. Aulbur, L. Jönsson, and J. Wilkins, *Quasiparticle Calculations in Solids*, edited by H. Ehrenreich (Academic, Orlando, 1999), Vol. 54 .

[17] Atomic units are used throughout this paper.

[18] H. N. Rojas, R. W. Godby and R. J. Needs, Phys. Rev. Lett. **74**, 1827 (1995); M. M. Rieger, L. Steinbeck, I.D. White, H. N. Rojas and R. W. Godby, Comput. Phys. Commun. **117**, 211 (1999).

[19] F. Chandezon, S. Bjørnholm, J. Borggreen and K. Hansen, Phys. Rev. B **55**, 5485 (1997).

[20] S. Saito, S. B. Zhang, S. G. Louie and M. L. Cohen, Phys. Rev. B **40**, 3643 (1989); J. Phys.: Condens. Matter **2**, 9041 (1990).

[21] An ideal image state is bound by the image potential. We therefore identify any bound state that is predominantly localized in the vacuum and that has an insignifcant overlap with the cluster region as an image state.

[22] The notation Na_m denotes a jellium cluster with r_s=4.0 and m valence electrons. The labels N and L refer to the radial and the angular quantum number, respectively, beginning with N=1 for every L.

[23] M. S. Hybertsen and S. G. Louie, Phys. Rev. B **34**, 5390 (1985); R. W. Godby, M. Schlüter and L. J. Sham, *ibid.* **37**, 10159 (1988).

[24] O. Pulci, L. Reining, G. Onida, R. DelSole and F. Bechstedt, Comput. Mater. Sci. **20**, 300 (2001).

[25] P. A. Serena, J. M. Soler and N. García, Phys. Rev. B **34**, 6767 (1986); E. V. Chulkov, V. M. Silkin and P. M. Echenique, Surf. Sci. Lett. **391**, 1217 (1997).